

## Single-Wall Carbon Nanotube Conducting Probe Tips

Neil R. Wilson,<sup>†</sup> David H. Cobden,<sup>†,‡</sup> and Julie V. Macpherson<sup>\*,§</sup>

Department of Physics, University of Warwick, Coventry CV4 7AL, U.K., Department of Physics, University of Washington, Seattle, Washington 98198-31560, and Department of Chemistry, University of Warwick, Coventry CV4 7AL, U.K.

Received: July 22, 2002; In Final Form: October 3, 2002

We describe a method for producing and characterizing electrically connected single-wall carbon nanotube scanned-probe tips. The stable contact resistance, of the order of 100 k $\Omega$ , makes these tips suitable for conducting probe applications. The nanotubes, grown by chemical vapor deposition, are mounted on the end of metal-coated (gold and platinum) silicon tips, using the “pick-up” method. Electrical characterization is carried out by lowering the tube into a liquid mercury contact and measuring the current through the tube as a function of applied bias voltage and immersion depth. This allows assessment of the magnitude and stability of the contact resistance, as well as identification of metallic and semiconducting tubes. It also offers a new geometry for investigating the transport properties of a nanotube as a continuous function of its conducting length.

### Introduction

Single-wall carbon nanotubes (SWNTs) exhibit remarkable electrical and mechanical properties. In particular, they behave as one-dimensional (1D) conductors, which can either be metallic or semiconducting. Metallic SWNTs have extremely low resistivity, and a single tube can sustain a current of tens of microamps.<sup>1</sup> SWNTs have also demonstrated significant promise as atomic force microscopy (AFM) tips.<sup>2</sup> “Tube tips” offer important advantages over conventional silicon microfabricated probes, including increased lateral resolution due to the small tube diameter ( $\sim 1$ – $2$  nm), a high aspect ratio, and damage resistance resulting from reversible elastic buckling.<sup>3</sup> Also, through selective chemical modification of the free end of the nanotube,<sup>4,5</sup> tube tips can be employed to probe the functionality of surface chemical groups and biological molecules.

Electrically connected tube tips hold considerable promise for conducting probe techniques, such as scanning tunneling microscopy (STM), electrostatic force microscopy (EFM), and scanned gate microscopy. Also, an electrically contacted SWNT represents an ideal geometrically well-defined nanometer-size electrode. Existing methodologies for fabricating small electrodes involve microwire etching and insulator deposition, which leave only the end of the sharp tip exposed.<sup>6,7</sup> Using this procedure, it is very difficult to determine the exact electrode geometry. In addition, the very high aspect ratio of a SWNT opens up the possibility of inserting a nanoscale electrode into small, deep pore structures or through a membrane with little disruption.

To date, however, there has been little work exploiting the electrical properties of SWNT tube tips. EFM has been performed with multiwalled nanotubes (MWNTs) attached to silicon AFM probes using nonconductive adhesive.<sup>8</sup> Electrochemical measurements have been made with MWNTs of diameter ca. 100 nm.<sup>9</sup> There have also been limited reports on

their use in STM,<sup>10–12</sup> where electrical contact was made either by bonding a MWNT to a silicon tip using carbon-tape adhesive<sup>12</sup> or by directly attaching the MWNT to an electrochemically sharpened tungsten<sup>10</sup> or gold-coated tungsten tip.<sup>11</sup> However, reliable spectroscopic analysis was not demonstrated. This was attributed to a poor electrical contact between tube and tip.<sup>10</sup> To the best of our knowledge there have been no methodical investigations of the magnitude and stability of the contact resistance of nanotubes mounted on tips.

In this Letter we describe a procedure for the reliable attachment of SWNTs to metal-coated (platinum and gold) AFM tips with a low-resistance electrical contact. The contact is characterized by dipping the tube tip into a liquid mercury electrode. The mercury makes an excellent sliding contact with the free end of the tube, consistent with the results of Frank et al.<sup>13,14</sup> on MWNTs. This procedure allows us to measure the electrical characteristics of a tube tip in detail, discriminate between metallic and semiconducting tubes, detect the presence of multiple tubes, and separate the contact resistance from the bulk resistivity.

### Experimental Section

**Fabrication of Electrically Connected Tube Tips.** Silicon AFM tips (FESP: Nanosensors) were metal coated with either an evaporated layer of gold (50 nm thick with a 10 nm adhesion layer of titanium) or a sputtered coating of platinum (50 nm thick, with a 5 nm adhesion layer of chromium). SWNTs were grown on a SiO<sub>2</sub> substrate using iron catalyst (ferric nitrate nonahydrate: Aldrich Chemicals) by chemical vapor deposition.<sup>15</sup> The substrates were placed in a 1 in. tube furnace and annealed under a flow of 600 standard cubic centimeters per minute (scm) Ar and 400 scm H<sub>2</sub> for 10 min at 850 °C. C<sub>2</sub>H<sub>4</sub> was then added at 2 scm for a further 10 min. Finally, the substrates were cooled under Ar. Cross-sectional analysis of tapping mode AFM images of the nanotube substrate revealed a height distribution between 0.8 and 3.0 nm. Micro-Raman characterization also demonstrated that most of the nanotubes

<sup>†</sup> Department of Physics, University of Warwick.

<sup>‡</sup> University of Washington.

<sup>§</sup> Department of Chemistry, University of Warwick.

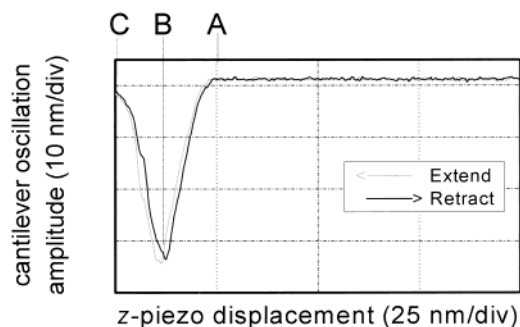


**Figure 1.** Cantilever oscillation amplitude versus  $z$ -piezo displacement for a long ( $L > 500$  nm) tube tip. The extend and retract characteristics show very little hysteresis, indicating a stable mounting of the nanotube on the tip. (A) marks the point of initial contact between the nanotube and the silicon substrate; at (B) the tube buckles until at (C) the oscillation amplitude returns to almost its free value.

were single walled,<sup>16</sup> with radial breathing mode wavenumbers consistent with nanotube diameters in the above range.

The nanotubes were attached to the metallized tips using the “pick-up”<sup>15</sup> method, in which the tip is scanned in tapping mode over the substrate and vertically oriented tubes adhere to it by van der Waals interactions.<sup>15</sup> Note that the widely used alternative technique of direct growth of tubes onto the tip<sup>17</sup> is incompatible with the metal coatings employed here. The resulting tube tips were observed in a low-resolution transmission electron microscope (TEM), which allowed assessment of the protruding length,  $L$ , and the arrangement of the nanotubes. In some cases a single nanotube was attached to the tip; in others, a few nanotubes were present, their protruding parts usually sticking together to form a small bundle.

For the electrical transport measurements described here, longer tube tips were selected ( $L > 200$  nm) to record the current response as a function of immersion depth in the mercury drop. The majority of these were found to be capable of topographical imaging. As expected, the shorter the nanotube tip the greater the improvement in image resolution due to the increased stiffness of the nanotube. Information about  $L$  and the stability of the nanotube’s mounting on the tip can be obtained by recording the amplitude and deflection of the cantilever as the tip is brought toward and away from the silicon substrate.<sup>18</sup> Figure 1 displays a typical trace of cantilever oscillation amplitude vs  $z$ -piezo displacement,  $d$  (increasing away from the substrate), for a long tube tip ( $L > 500$  nm). As  $d$  is reduced, the amplitude starts to decrease when the end of the nanotube comes into contact with the substrate (point A in Figure 1). When the force on the nanotube reaches a critical value (point B), the tube buckles and thereafter the amplitude returns almost to its free value (point C). The larger  $L$  is, the lower the critical force and the more quickly the amplitude recovers. A consistent, reproducible amplitude–displacement curve is indicative of a stable tube tip.

**Electrical Characterization.** For the electrical measurements the AFM (Digital Instruments Multimode IIIa) was shielded using a home-built Faraday cage. The AFM probe was held in an EFM holder, which allowed a voltage,  $V_{\text{tip}}$ , to be applied to the tip. A  $50 \mu\text{m}$  diameter hemisphere of mercury, formed by the electrochemical reduction of  $\text{Hg}_2^{2+}$  at a  $50 \mu\text{m}$  diameter platinum disk ultramicroelectrode,<sup>19</sup> functioned as the liquid metal contact. An optical image of the setup is shown in Figure 2a.

The nanotube tip was first lowered toward the liquid metal using the  $z$ -stepper motor in increments less than  $L$ . A sudden change in the deflection signal of the cantilever occurs when

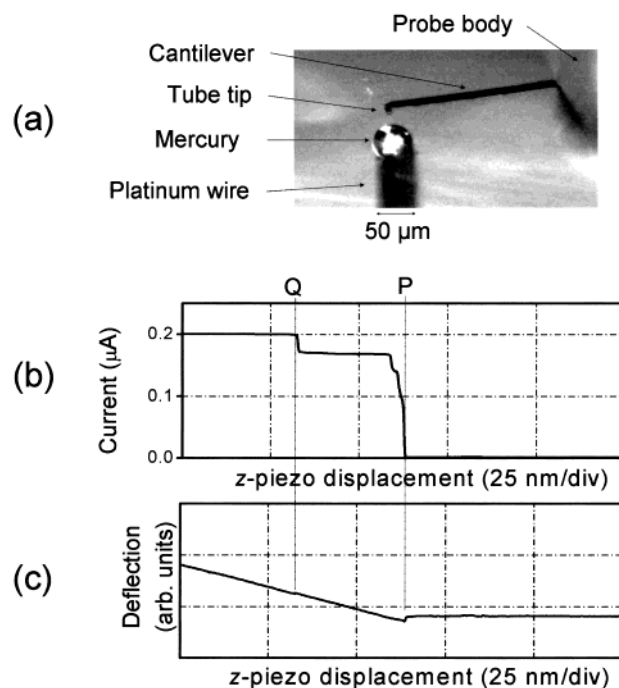


**Figure 2.** (a) Optical microscope image of the cantilever, tube tip, and mercury drop arrangement. (b) Current– and (c) deflection–distance characteristics for a platinum tube tip bundle, as the tip was brought toward and into contact with the liquid mercury. The tip was held at a constant voltage of  $-25$  mV. The steplike increases in current at P and Q coincide with dips in the cantilever deflection, as indicated by the dashed lines. These mark the penetration of successive conducting nanotubes into the mercury drop.

the tube first encounters the mercury surface. The  $z$ -piezo is then used to precisely control  $d$ .  $V_{\text{tip}}$  was controlled by a PC data acquisition card. The current,  $i$ , was converted to a voltage by a virtual-earth current preamplifier (DL Instruments Model 1211), and the resulting signal fed to an auxiliary input on the AFM controller using a signal access module. This allowed the simultaneous measurement of current and tip deflection (force) as a function of  $d$ .

## Results and Discussion

Electrical measurements were carried out with both platinum and gold tube tips. The current flowing through the tube tip was initially measured as a function of  $d$ , in the linear response regime using a fixed  $V_{\text{tip}}$  ( $-25$  mV). Parts b and c of Figure 2 show typical traces of current and deflection against  $d$  for a platinum tube tip bundle. As  $d$  is steadily decreased, the current suddenly rises from zero at the same point (P) as a small attractive force is observed. The current then rises in steps through a series of plateaus, whereas the force becomes repulsive and grows linearly. We often notice a small dip in the force at each current step, as for instance at point Q. For most bundles, the characteristics are highly reproducible. With only one nanotube on the tip, a single current plateau is observed, but the step is not well behaved, probably as a result of its lower rigidity. For EFM and scanned gate microscopy applications, where longer tube tips are desired in view of the long-range forces, the more rigid tube bundles will also give higher spatial resolution due to their lower thermal fluctuations.

Although the force response is not yet fully understood, the origin of the current steps and plateaus is clear. When gold-coated tips are used, if the gold coating touches the mercury, it quickly dissolves (as confirmed by subsequent TEM imaging) and the current vanishes. For platinum tips, if the platinum

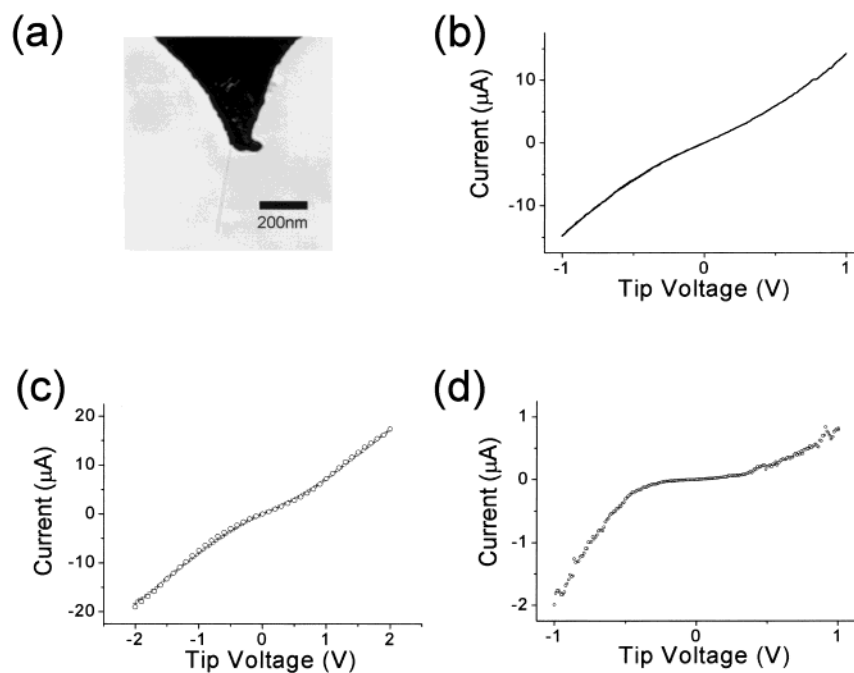


**Figure 3.** (a) TEM image of a gold tube tip. The poor resolution prohibits assessment of the diameter of the tube but allows a reasonable measurement of the protruding length. (b)  $i$ - $V_{\text{tip}}$  response of the tube tip depicted in (a), indicative of metallic nanotube. (c)  $i$ - $V_{\text{tip}}$  traces for another gold tube tip, recorded under identical conditions 3 hours apart, illustrating the stability of the system. (d)  $i$ - $V_{\text{tip}}$  response of a gold tube tip, showing behavior indicative of a semiconducting nanotube.

touches the mercury, a stable, very high conductance metal-metal contact is established. The movement of mercury along the tube to short to the tip is highly unlikely, as mercury does not wet carbon nanotubes.<sup>20</sup> Therefore, the current must flow through the nanotubes. Each current step is produced when a conducting tube penetrates the mercury. The existence of plateaus between the steps implies that the nanotube resistivity is small, as discussed below. The multiple features at the first current step in Figure 2b (point P) may be due to several tubes in a bundle penetrating the mercury in close succession.

With our limited TEM resolution we could not determine whether the Fe catalyst particle remains attached to the free end of the nanotube after pick up. However, this is unlikely to influence the transport measurements, as the tube end is always fully immersed in the mercury during current measurements.

To further characterize the nanotube tips,  $i$ - $V_{\text{tip}}$  traces were recorded at fixed  $d$ , on a stable plateau. Figure 3a is a TEM image of a gold tube tip with a single protruding nanotube. The deformity of the apex is probably a result of abrasion of the soft gold coating during scanning and has no consequences for the performance of the tube tip. Figure 3b displays the  $i$ - $V_{\text{tip}}$  response of this tube tip with ca. 50 nm of the tube immersed in the mercury. The corresponding  $i$ - $d$  response showed a very stable, single plateau. The  $i$ - $V_{\text{tip}}$  trace is highly symmetric, with a low-bias ohmic resistance of ca. 170 k $\Omega$ . The observed characteristics are consistent with a metallic nanotube.<sup>21</sup> Importantly for our intended applications, for all such metallic nanotube tips, the  $i$ - $d$  and  $i$ - $V_{\text{tip}}$  responses are very stable, for  $V_{\text{tip}}$  as high as 4 V and  $i$  up to 50  $\mu\text{A}$ . The stability is illustrated in Figure 3c, which shows two almost identical  $i$ - $V_{\text{tip}}$  traces, recorded 3 hours apart for a gold tube tip.

Figure 3d shows an  $i$ - $V_{\text{tip}}$  trace for another gold tube tip on an  $i$ - $d$  plateau. In this case, the trace is asymmetric and highly nonlinear, with a much higher resistance at low bias of  $\sim 10$  M $\Omega$ . This is the behavior expected of a semiconducting nanotube,<sup>1</sup> where Schottky barriers exist at both the metal contacts, which suppress the low-bias conductance.<sup>22</sup> The

asymmetry can be attributed to the difference between the mercury and the gold contacts. Semiconducting nanotubes are normally p-doped by adsorbates.<sup>1</sup> The current should be largest when holes are injected into the nanotube from the contact with the lowest Schottky barrier, i.e., when that contact is positively biased. Because the current is found to be larger for a positive bias on the mercury, the implication is that the Schottky barrier to the mercury is smaller than that to the gold. This is consistent with the work function of Au (5.1 eV) being greater than that of mercury (4.5 eV).<sup>23</sup>

A metallic SWNT with perfect contacts has a theoretical minimum possible resistance of 6.5 k $\Omega$ .<sup>24</sup> In general, we obtained plateau resistances (from  $i$ - $d$  traces) in the range 100–200 k $\Omega$ , for metallic nanotubes. Note, for each nanotube tip we are able to accurately determine this value. The approximate flatness of each plateau implies that the intrinsic resistance of the nanotube, which should be proportional to its exposed length, is small compared with the resistance of one or both contacts. Given that mercury makes excellent electrical contact with multiwall carbon nanotubes,<sup>13</sup> it is likely the measured resistance is dominated by the nanotube-tip contact. In fact, resistances in the same range 100–200 k $\Omega$  are also obtained when nanotubes are laid on top of prefabricated gold electrodes.<sup>21</sup> We found that it was easier to obtain reproducible lower resistance plateaus with gold than platinum. This was attributed primarily to the smoother gold tip coating, as observed in the TEM, which should result in a greater contact area between the nanotube and the metal.

Closer inspection of the  $i$ - $d$  plateaus reveals that they have a small slope. Because the nanotube-tip contact is unlikely to depend on  $d$ , this slope could come either from a gradual change in the mercury-nanotube contact or from a changing resistance of the exposed length of nanotube. Once the immersed length of the nanotube exceeds some characteristic value we would expect no further variation in the mercury-nanotube contact resistance. Experiments on multiwall nanotubes<sup>13,14</sup> imply that this length is very small and that the mercury contact is nearly

ideal for even a few nanometers of nanotube immersed. Therefore we believe the slope gives a direct measure of the resistance per unit length of the nanotube, although future measurements of the precise functional dependence of the resistance on depth will be needed to confirm this. Our preliminary investigations on single nanotubes yield a resistance per unit length in the range 1–5 k $\Omega$   $\mu\text{m}^{-1}$ .<sup>25</sup> This result is consistent with other indications<sup>24,26</sup> that metallic nanotubes are nearly ballistic conductors over several hundred nanometers at room temperature.

## Conclusions

Attachment of SWNTs to metal-coated AFM tips by van der Waals forces produces mechanically and electrically stable, conducting tube tips, capable of high-resolution topographical imaging, with contact resistances to metallic tubes as low as 100 k $\Omega$ . These are key requirements for the application of tube tips as electrical and electrochemical scanned probes, research areas that we are currently exploring. Dipping the end of the nanotube into liquid mercury and measuring the electrical characteristics as a function of immersion depth allows the electrical nature of the tube and its contact to the tip to be assessed. Furthermore, this procedure opens up new possibilities for investigating the length dependence of the electrical transport properties of individual nanotubes.

**Acknowledgment.** J.V.M. thanks the Royal Society for the award of a University Research Fellowship. We also thank the EPSRC for support (studentship for N.R.W. and the purchase of an AFM under the Strategic Equipment Initiative). We are grateful to Steve York (Department of Physics, University of Warwick) for help with TEM, Prof. Robert Young (Manchester Materials Science Centre, UMIST) for assistance with the Micro-Raman, and Dr. Boris Mouzykantskii (Department of Physics, University of Warwick) for many interesting discussions. We also thank Dr. Barry Cheung and Prof. Charles Lieber (Department of Chemistry, Harvard University) for much valuable advice on growth and the production of nanotube-AFM tips.

## References and Notes

(1) Saito, R.; Dresselhaus, G.; Dresselhaus, M. S. *Physical Properties of Carbon Nanotubes*; Imperial College Press: London, 1998.

- (2) (a) Wong, S. S.; Woolley, A. T.; Odom, T. W.; Huang, J.-L.; Kim, P.; Vezenov, D. V.; Lieber, C. M. *Appl. Phys. Lett.* **1998**, *73*, 3465. (b) Wong, S. S.; Harper, J. D.; Lansbury, P. T.; Lieber, C. M. *J. Am. Chem. Soc.* **1998**, *120*, 603.
- (3) Larsen, T.; Moloni, K.; Flack, F.; Eriksson, M. A.; Lagally, M. G.; Black, C. T. *Appl. Phys. Lett.* **2002**, *80*, 1996.
- (4) (a) Wong, S. S.; Joselevich, E.; Woolley, A. T.; Cheung, C. L.; Lieber, C. M. *Nature* **1998**, *394*, 52. (b) Wong, S. S.; Woolley, A. T.; Joselevich, E.; Cheung, C. L.; Lieber, C. M. *J. Am. Chem. Soc.* **1998**, *120*, 8557.
- (5) Yang, Y.; Zhang, J.; Nan, X.; Liu, Z. *J. Phys. Chem. B* **2002**, *106*, 4139.
- (6) Penner, R. M.; Heben, M. J.; Lewis, N. J. *Anal. Chem.* **1989**, *61*, 1630.
- (7) Slevin, C. J.; Gray, N. J.; Macpherson, J. V.; Webb, M. A.; Unwin, P. R. *Electrochem. Commun.* **1999**, *1*, 282.
- (8) Arnason, S. B.; Rinzler, A. G.; Hudspeth, Q.; Hebard, A. F. *Appl. Phys. Lett.* **1999**, *75*, 2842.
- (9) Campbell, J. K.; Sun, L.; Crooks, R. M. *J. Am. Chem. Soc.* **1999**, *121*, 3779.
- (10) Shimizu, T.; Tokumoto, H.; Akita, S.; Nakayama, Y. *Surf. Sci.* **2001**, *486*, L455.
- (11) Watanabe, H.; Manabe, C.; Shigematsu, T.; Shimizu, M. *Appl. Phys. Lett.* **2001**, *78*, 2928.
- (12) Dai, H.; Hafner, J. H.; Rinzler, A. G.; Colbert, D. T.; Smalley, R. E. *Nature* **1996**, *384*, 147.
- (13) Frank, S.; Poncharal, P.; Wang, Z. L.; de Heer, W. A. *Science* **1998**, *280*, 1744.
- (14) Poncharal, P.; Frank, S.; Wang, Z. L.; de Heer, W. A. *Eur. Phys. J. D* **1999**, *9*, 77.
- (15) Hafner, J. H.; Cheung, C. L.; Oosterkamp, T. H.; Lieber, C. M. *J. Phys. Chem. B* **2001**, *105*, 743.
- (16) Jorio, A.; Saito, R.; Hafner, J. H.; Lieber, C. M.; Hunter, M.; McClure, T.; Dresselhaus, G.; Dresselhaus, M. S. *Phys. Rev. Lett.* **2001**, *86*, 1118.
- (17) Hafner, J. H.; Cheung, C. L.; Lieber, C. M. *J. Am. Chem. Soc.* **1999**, *121*, 9750.
- (18) Cheung, C. L.; Hafner, J. H.; Lieber, C. M. *Proc. Natl. Acad. Sci. U.S.A.* **2000**, *97*, 3809.
- (19) Wehmeyer, K. R.; Wightman, R. M. *Anal. Chem.* **1985**, *57*, 1989.
- (20) Dujardin, E.; Ebbesen, T.; Hiura, H.; Tanigaki, K. *Science* **1994**, *265*, 1850.
- (21) Yao, Z.; Kane, C. L.; Decker, C. *Phys. Rev. Lett.* **2000**, *84*, 2941.
- (22) See for example: Appenzeller, J.; Knoch, J.; Derycke, V.; Martel, R.; Wind, S.; Avouris, Ph. *Phys. Rev. Lett.* **2002**, *89*, 126801.
- (23) Roderick, E. H.; Williams, R. H. *Metal-Semiconductor Contacts*; Oxford University Press: Oxford, U.K., 1988.
- (24) White, C. T.; Todorov, T. N. *Nature* **1998**, *393*, 240.
- (25) Wilson, N. R.; Macpherson, J. V.; Cobden, D. H. Manuscript in preparation.
- (26) De Pablo, P. J.; Gomez-Navarro, C.; Martinez, M. T.; Benito, A. M.; Maser, W. K.; Colchero, J.; Gomez-Herrero, J.; Baro, A. M. *Appl. Phys. Lett.* **2002**, *80*, 1462.